Tetrahedron 67 (2011) 891–897

Contents lists available at ScienceDirect

Tetrahedron

journal homepage: www.elsevier.com/locate/tet

Colorimetric response of spiropyran derivative for anions in aqueous or organic media

Yasuhiro Shiraishi *, Masataka Itoh, Takayuki Hirai

Research Center for Solar Energy Chemistry, and Division of Chemical Engineering, Graduate School of Engineering Science, Osaka University, 1-3 Machikaneyama-cho, Toyonaka 560-8531, Japan

ARTICLE INFO

Article history:
Received 3 November 2010
Received in revised form 6 December 2010
Accepted 7 December 2010
Available online 17 December 2010

Keywords:
Spiropyran
Receptor
Optical sensing
Anions
Water

ABSTRACT

We previously found that a simple spiropyran derivative (**1**:1′,3′,3′-trimethyl-6-nitro-spiro-[2*H*-1-benzopyran-2,2′-indoline]) behaves as a selective and sensitive cyanide anion (CN^-) receptor in aqueous media under UV irradiation[13]. The receptor, when irradiated by UV light in a water/MeCN mixture, creates a CN^--selective absorption band via a nucleophilic addition of CN^- to **1** (formation of the **1**–CN^- species) and allows quantitative determination of very low levels of CN^-. In the present work, effects of pH and water content on the response of **1** to anions were studied to clarify the detailed properties of **1**. In aqueous media, **1** reacts selectively with CN^- regardless of pH and water content, but the reaction is suppressed by a decrease in pH and an increase in water content due to the protonation of CN^-. In contrast, in pure MeCN, addition of F^- also creates a new absorption band, as does CN^-. This is promoted via a nucleophilic interaction between **1** and F^- in a 1:2 stoichiometry (formation of the **1**–$2F^-$ species). The **1**–CN^- and **1**–$2F^-$ species have different photochemical properties; the **1**–CN^- species is stable upon UV irradiation, while the UV irradiation of the **1**–$2F^-$ species leads to a decomposition of the spiropyran platform.

1. Introduction

Anions play important roles in the areas of biological and environmental chemistry. The design of receptors that selectively detect the targeted anions has therefore attracted a great deal of attention.[1] Various receptors have been proposed for selective detection of anions, such as fluoride (F^-),[2] chloride (Cl^-),[3] acetate (AcO^-),[4] dihydrogenphosphate ($H_2PO_4^-$),[5] and hydrogensulfate (HSO_4^-).[6] In particular, the cyanide anion (CN^-) receptors have attracted much attention because CN^- is extremely toxic to living organisms.[7] The maximum permissive level of cyanide in drinking water is therefore set at 1.9 μM by the World Health Organization (WHO).[8] Several kinds of CN^- receptors have been proposed, but many of these rely on a hydrogen-bonding motif and act only in organic media.[9] To overcome this limitation, reaction-based CN^- receptors have been proposed;[10–12] however, many of these display relatively poor selectivity[10] and a high detection limit (>1.9 μM)[11] in aqueous media. There are only a few reports of CN^- receptors with high selectivity and sensitivity in aqueous media.[12]

Earlier, we reported that a simple spiropyran derivative (**1**:1′,3′,3′-trimethyl-6-nitro-spiro-[2*H*-1-benzopyran-2,2′-indoline]), a photochromic compound, behaves as a highly selective and sensitive CN^- receptor in aqueous media under UV irradiation (Scheme 1).[13] The colorless spirocyclic (SP) form of **1**, when irradiated by UV light in a water/MeCN (50/50 v/v) mixture, is converted to the colored merocyanine (MC) form with an absorption band at 450–550 nm. The nucleophilic addition of CN^- to the positively-charged spirocarbon of the MC form of **1** leads to a formation of the **1**–CN^- species with a blue-shifted absorption at 350–500 nm. This thus enables quantification of very low levels of CN^- (>1.7 μM) by absorption analysis.

The purpose of the present work is to clarify the detailed properties of the receptor **1** for anions. The effects of pH and water content of the solution on the response of **1** to anions have been studied. In aqueous media, **1** reacts selectively with CN^- regardless of pH and water content, but the reaction is suppressed by a decrease in pH and an increase in water content. In contrast, in pure MeCN, addition of F^- to **1** also creates a blue-shifted absorption as does CN^-. This is promoted via a nucleophilic interaction between **1** and F^- in a 1:2 stoichiometry (formation of the **1**–$2F^-$ species) (Scheme 1). We also describe here the different properties of the **1**–CN^- and **1**–$2F^-$ species upon UV irradiation.

2. Result and discussion

2.1. Effect of pH

The change in absorption spectra of **1** in aqueous media with basic pH has already been described in the previous work,[13] and a brief description is made here. Fig. 1a shows the absorption spectra of **1** (20 μM) measured in a buffered water/MeCN (50/50 v/v)

* Corresponding author. Tel.: +81 6 6850 6271; fax: +81 6 6850 6273; e-mail address: shiraish@cheng.es.osaka-u.ac.jp (Y. Shiraishi).

0040-4020/$ – see front matter © 2010 Elsevier Ltd. All rights reserved.
doi:10.1016/j.tet.2010.12.021

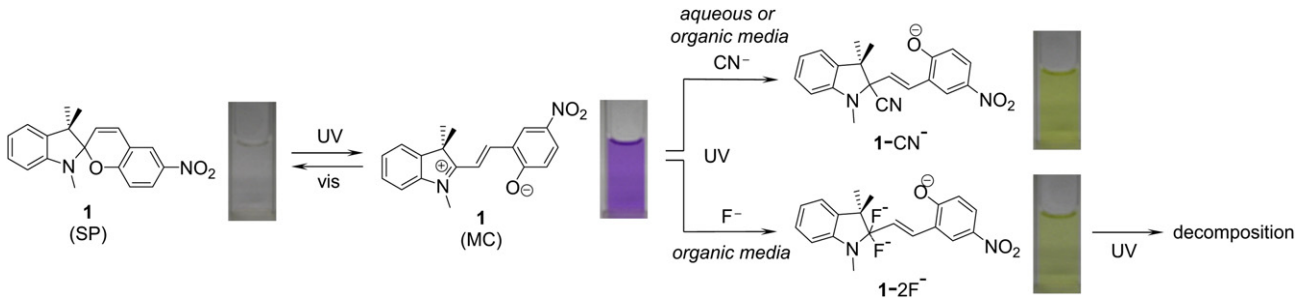

Scheme 1. Structure and color change of **1** in the presence of CN^- or F^- under UV irradiation.

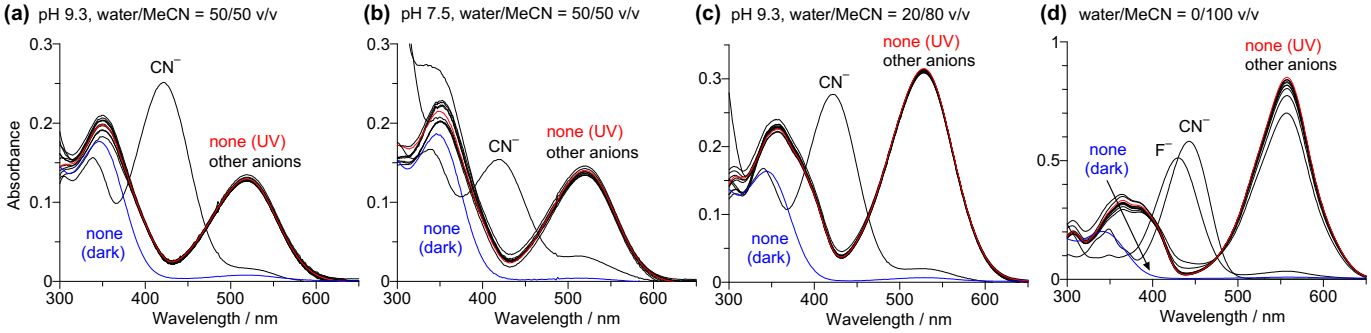

Fig. 1. Absorption spectra of **1** (20 μM) measured in buffered water/MeCN mixtures with different pH and compositions at 25 °C. (a) pH 9.3 (CHES 100 mM), 50/50 v/v, (b) pH 7.5 (HEPES 100 mM), 50/50 v/v, (c) pH 9.3, 20/80 v/v, and (d) 0/100 v/v. The blue spectra were obtained without anion in the dark. The red spectra were obtained without anion under UV irradiation (334 nm, 5 min). The black spectra were obtained with each respective anion (F^-, Cl^-, Br^-, I^-, AcO^-, $H_2PO_4^-$, HSO_4^-, ClO_4^-, NO_3^-, SCN^-, or CN^-) under UV irradiation for 30 min, where 50 equiv of anion was added to the samples a, c, and d, and 500 equiv of anion was added to the sample b.

mixture with pH 9.3 in the presence of 50 equiv of respective anion as an *n*-tetrabutylammonium salt.[13] As shown by blue line, without anion in the dark, **1** shows almost no absorption in the visible region, indicating that **1** exists as an SP form. As shown by red line, UV irradiation (334 nm) of the sample leads to a generation of the absorption band at 450–650 nm, assigned to the MC form. Addition of CN^- to the solution under UV irradiation leads to a decrease in the MC band along with an appearance of new absorption band at 350–500 nm, assigned to the **1**–CN^- species (Scheme 1). In contrast, addition of other anion (F^-, Cl^-, Br^-, I^-, AcO^-, $H_2PO_4^-$, HSO_4^-, ClO_4^-, NO_3^-, or SCN^-) does not show any spectral change. Fig. 1b shows the change in absorption spectra of **1** measured in a buffered water/MeCN (50/50 v/v) mixture at pH 7.5. The spectral change upon UV irradiation and addition of anions is similar to that observed at pH 9.3 (Fig. 1a). This suggests that the receptor **1** selectively detects CN^- even at neutral pH.

Fig. 2a shows the result of absorption titration of **1** with CN^- in a water/MeCN (50/50 v/v) mixture at pH 9.3 under UV irradiation. The CN^- addition leads to a continuous decrease in the 519 nm MC band, along with an increase in the 421 nm **1**–CN^- band. The absorbance increase is saturated upon addition of 30 equiv of CN^-. The receptor **1** associates with CN^- in a 1:1 stoichiometry. This is confirmed by a non-linear fitting of the titration data. As described previously,[13] when assuming a 1:1 association between **1** and CN^-, the relationship between the absorbance of the MC form and the CN^- concentration is expressed as follows:

$$A = A_0 + \frac{A_{\max} - A_0}{[\mathbf{1}]_0} \times \frac{C - \sqrt{C^2 - 4[\mathbf{1}]_0\left[CN^-\right]_0}}{2} \quad (1)$$

$$C = [\mathbf{1}]_0 + \left[CN^-\right]_0 + \frac{1}{K_{ass}} \quad (2)$$

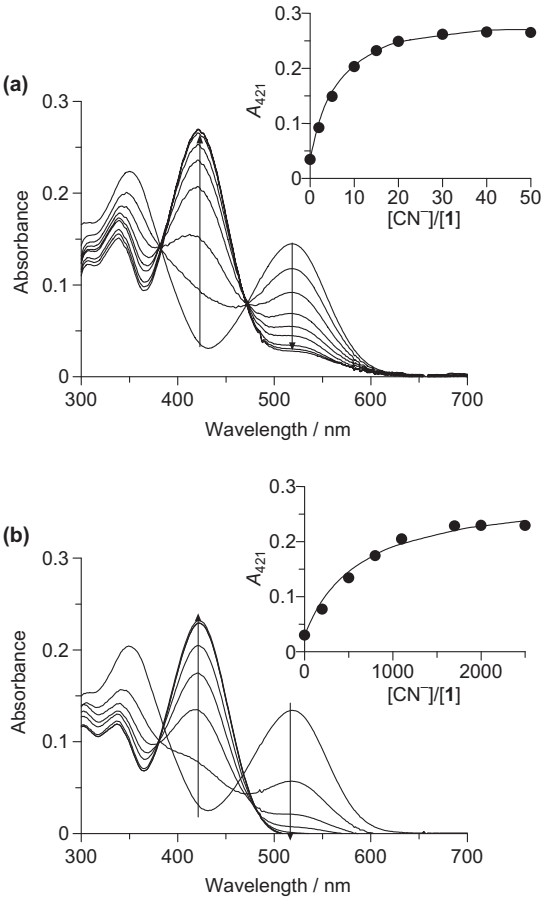

Fig. 2. Absorption titration of **1** (20 μM) with CN^- in a buffered water/MeCN (50/50 v/v) mixture with (a) pH 9.3 and (b) pH 7.5 under UV irradiation at 25 °C. (inset) Change in MC band absorbance, where the lines are the non-linear fitting curves obtained assuming a 1:1 association with **1** and CN^-.

where $[\mathbf{1}]_0$ and $[CN^-]_0$ are the initial concentrations of **1** and CN^-, respectively, A_0 is the absorbance of **1** obtained without anion, A is the absorbance of **1** obtained with CN^-, A_{max} is the absorbance of **1** obtained with excess amount of CN^-, and K_{ass} is the association constant. As shown by the line in inset of Fig. 2a, the titration data are fully explained with the calculated curve, indicating that **1** indeed associates with CN^- in a 1:1 stoichiometry. The association constant, K_{ass}, is determined to be 9.8×10^3 M^{-1} (Table 1).

CN^- and F^- in MeCN. The 427 nm band is blue-shifted as compared to the **1**–CN^- band (443 nm), indicating that the interaction of **1** with F^- produces the species with a different electronic state.

Effect of water content on the association constant between **1** and CN^- was studied. As shown in Table 1, K_{ass} in pure MeCN is 5.5×10^6 M^{-1}, but the value decreases with an increase in water content: 2.5×10^4 (10/90 v/v water/MeCN)>9.8×10^3 (50/50 v/v)> 6.0×10^3 (70/30 v/v). This indicates that the reaction of **1** with CN^- is

Table 1
The first-order rate constant (k), activation energy (E_a), and association constant (K_{ass}) for interaction between **1** and CN^- or F^- in a water/MeCN mixture

Anion	Water/MeCN/v/v	pH	E_a/kJ mol^{-1} [a]	T/°C	K_{ass}	k/s^{-1}
CN^-	70/30	9.3	33.1±14.5	15		6.66×10^{-4} [c]
				25	$(6.00\pm0.50)\times10^3$ M^{-1} [b]	8.50×10^{-4} [c]
				40		1.97×10^{-3} [c]
	50/50	9.3	26.9±1.1	15		1.70×10^{-3} [c]
				25	$(9.80\pm0.20)\times10^3$ M^{-1}	2.44×10^{-3} [c]
				40		4.17×10^{-3} [c]
		7.5		25	80.0±0.7 M^{-1}	
	10/90	9.3	9.4±4.5	15		3.74×10^{-3} [c]
				25	$(2.50\pm0.30)\times10^4$ M^{-1} [b]	4.57×10^{-3} [c]
				40		5.15×10^{-3} [c]
	0/100			15		>2.87×10^{-2} [d]
				25	$(5.50\pm0.50)\times10^6$ M^{-1} [b]	
F^-	0/100		25.6±10.6	15		1.43×10^{-2} [e]
				25	$(1.83\pm0.11)\times10^8$ M^{-2}	2.40×10^{-2} [e]
				40		3.40×10^{-2} [e]

[a] The Arrhenius plot of the kinetic data are summarized in Fig. S4 (Supplementary data).
[b] The absorption titration data for these samples are summarized in Fig. S1 (Supplementary data), where the non-linear fitting results are also shown.
[c] The kinetic absorption data are summarized in Fig. S2 (Supplementary data).
[d] The reaction of **1** with CN^- terminates within 1 min, and the accurate rate constant cannot be determined.
[e] The kinetic absorption data are summarized in Fig. S3 (Supplementary data).

Fig. 2b shows the absorption titration results obtained at pH 7.5. The spectral change is similar to that obtained at pH 9.3 (Fig. 2a), but the change is saturated upon addition of 2000 equiv of CN^-. As shown in inset, the titration data are well explained by a calculated line, indicating that **1** associates with CN^- in a 1:1 stoichiometry even at neutral pH. The K_{ass} value is 80 M^{-1}, which is much lower than that obtained at pH 9.3 (9.8×10^3 M^{-1}). It is well known that CN^- is protonated in acidic or neutral pH, as follows.[11b]

$$H^+ + CN^- \rightleftarrows HCN \quad (pK_a = 9.2) \tag{3}$$

The protonation of CN^- at neutral pH therefore probably suppresses the reaction between **1** and CN^-, resulting in low association constant. The results indicate that the pH of solution does not affect the CN^- selectivity of **1**, but strongly affects the association strength.

2.2. Effect of water content

Fig. 1c and d show the absorption spectra of **1** measured in a 20/80 v/v water/MeCN mixture (pH 9.3) and pure MeCN, respectively. The absorption spectra obtained without anion (shown by blue and red line) are similar to that obtained in a 50/50 v/v mixture (Fig. 1a). It is noted that the MC absorption band generated by UV irradiation (red spectra) blue-shifts with an increase in water content; 0% solution shows a band at 560 nm, while 20 and 50% solutions show at 528 and 519 nm, respectively. This is because the MC form is stabilized by a hydrogen bonding interaction with water molecules.[14] In a 20/80 v/v water/MeCN solution (Fig. 1c), addition of anions show absorption change similar to that obtained in a 50/50 v/v mixture (Fig. 1a), indicating that **1** selectively detects CN^- regardless of water content. Absorption behavior in pure MeCN is, however, different. As shown in Fig. 1d, addition of F^- to **1** in MeCN also leads to an appearance of blue-shifted absorption at 427 nm, as does CN^-. This suggests that the MC form of **1** associates with both

suppressed by an increase in water content. This is because the protonation of CN^- occurs more significantly in a solution with a larger water content.

Effect of water content on the activation energy, E_a, of the reaction between **1** and CN^- was studied based on the kinetic absorption measurement. As described previously,[13] the first-order rate constant for reaction, k (s^{-1}), can be expressed with the absorbance of the **1**–CN^- species, as follows:

$$\ln\left(\frac{A_\infty - A_t}{A_\infty - A_0}\right) = kt \tag{4}$$

A_0, A_t, and A_∞ are the absorbance of the **1**–CN^- species at time 0, t, and infinity, respectively. The measurement was carried out with 50 equiv of CN^- to **1**. UV light was irradiated to the solution containing **1** for 5 min. CN^- was added to the solution, and the spectral measurement was started with continued UV irradiation. The kinetic absorption data obtained at different temperature are shown in Fig. S2 (Supplementary data), and the rate constants are summarized in Table 1. The rate constant increases with a decrease in water content of the solution, indicating that the protonation of CN^- affects strongly the reaction with **1**. In pure MeCN, the absorption change after CN^- addition terminates within 1 min, and the rate constant cannot be determined. The activation energy (E_a) of the interaction is determined with the Arrhenius equation, as follows:[13]

$$\ln k = \ln A - \frac{E_a}{RT} \tag{5}$$

Fig. S4 (Supplementary data) shows the Arrhenius plot of the kinetic data. As summarized in Table 1, E_a values increase with an increase in water content of the solution. This again suggests that the protonation of CN^- occurs more significantly in the solution with larger water content and suppresses the reaction of **1** with CN^-.

2.3. Response of 1 with F^- in MeCN

As shown in Fig. 1d, **1** dissolved in pure MeCN shows a blue-shifted absorption upon addition of F^- as well as CN^-. Fig. 3 shows the result of absorption titration of **1** with F^- in MeCN under UV irradiation. The stepwise F^- addition leads to a continuous decrease in the 560 nm MC band, along with an appearance of 427 nm absorption band. The isosbestic points at 397 and 472 nm suggest that the interaction of **1** with F^- produces a single component, as is the case for CN^-. However, the absorption titration result of **1** with F^- cannot be explained by a non-linear fitting obtained assuming a 1:1 association between **1** and F^-.

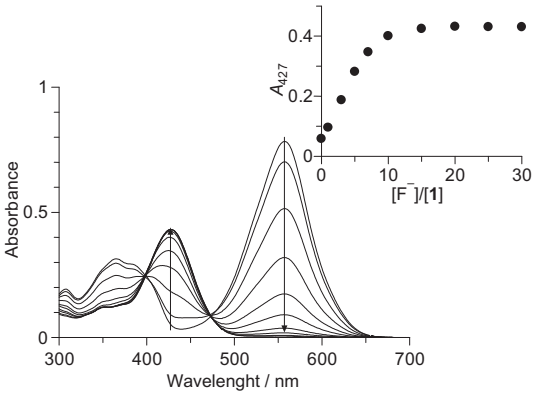

Fig. 3. Absorption titration of **1** (20 μM) with F^- in MeCN under UV irradiation at 25 °C. (inset) Change in absorbance at 427 nm.

Compound **1** associates with F^- in a 1:2 stoichiometry. This is confirmed by the Benesi–Hildebrand analysis[15] of the absorption titration data. When assuming a 1:*n* stoichiometry for association between **1** and F^-, the association constant, K_{ass}, is given by the following equation:

$$\frac{A_0}{A_0 - A} = \frac{1}{K_{ass}\left[F^-\right]_0^n} + 1 \qquad (6)$$

A_0 is the absorbance of **1** without anion, A is the absorbance of **1** obtained with F^-, and $[F^-]_0$ is the initial concentrations of F^-. As shown in Fig. 4, the plot of $A_0/(A_0-A)$ against $1/[F^-]_0^2$ shows a linear relationship, indicating that **1** associates with F^- in a 1:2 stoichiometry (formation of **1**–2F^- species). K_{ass} is determined from the slope to be 1.83×10^8 M^{-2}. Further confirmation of the 1:2 association is made by the Job's plot analysis; as shown in Fig. 5, the plot shows a maximum absorption at $X=[F^-]/([F^-]+[1])=0.667$. Kinetic absorption measurement for interaction between **1** and F^- was carried out (Fig. S3, Supplementary data). The rate constants

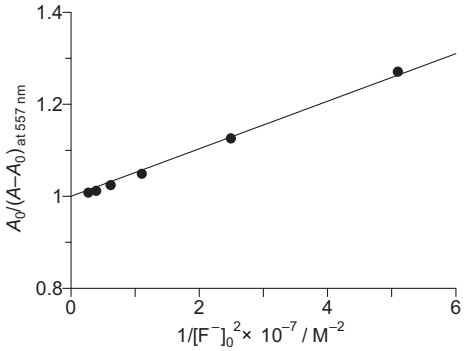

Fig. 4. Benesi–Hildebrand plot of the absorption titration data for association of **1** with F^- using Eq. (6), assuming a 1:2 stoichiometry (n=2). The plots assuming 1:1 and 1:3 stoichiometries are shown in Fig. S5 (Supplementary data).

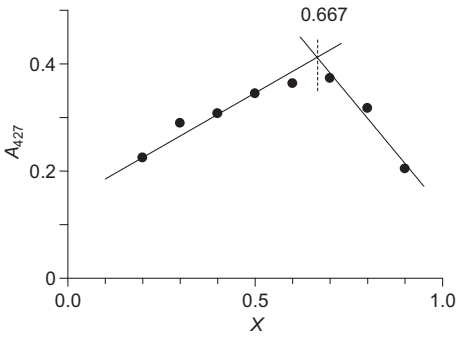

Fig. 5. Job's plot of **1** with F^- ($X=[F^-]/([F^-]+[1])$) in MeCN. The total concentration of **1** and F^- is 100 μM.

determined at different temperature are summarized in Table 1. E_a for this interaction is determined by the Arrhenius plot analysis to be 25.6 kJ mol^{-1}. In contrast, E_a for reaction between **1** and CN^- is<9.4 kJ mol^{-1}, indicating that the interaction of **1** with F^- is much weaker.

2.4. Structure of 1–CN^- and 1–2F^- species

The structure of the **1**–2F^- species must be clarified. Figs. 6 and 7 show the change in ^{1}H NMR spectra of **1** obtained by UV irradiation in the presence of CN^- and F^- for 10 min. Upon addition of both CN^- and F^-, large decrease in chemical shift (ca. −0.7 ppm) is observed for the H_g proton in the *ortho* position relative to the phenolate oxygen of **1**. This indicates that the interaction of **1** with both CN^- and F^- under UV irradiation produce a spirocycle-opened species.[16,12e] As reported,[17] the *N*-methyl protons of the MC form shift downfield as compared to the corresponding SP form due to the quaternarization of nitrogen atom. However, in the present case, addition of CN^- or F^- leads to an upfield shift of the *N*-methyl protons. This is because the interaction between the spirocarbon with CN^- or F^- suppresses the quaternarization of the nitrogen atom. These results indicate that, as is the case for CN^-,[13] F^- interacts with the spirocarbon of the MC form of **1** and produces a spirocycle-opened species.

To clarify the geometry of the **1**–2F^- species, ab initio calculations were performed at the DFT level within the Gaussian 03 program.[18] Fig. 8 shows the optimized geometry of the MC form of **1**, **1**–CN^-, and **1**–2F^- species, respectively. In the case of **1**–CN^- species, the distance between the spirocarbon of **1** and the C atom of CN^- is 1.50 Å, which is similar to the C–C covalent bond distance (1.53 Å).[19] This suggests that CN^- associates strongly with the spirocarbon. In the case of **1**–2F^- species, two F^- atoms are located at the top and bottom side of the spirocarbon of the indole plane. The average distance between the spirocarbon and F^- is 2.36 Å, which is much larger than the C–F covalent bonding distance (1.39 Å) but smaller than the sum of the van der Waals radii of C and F^- (3.54 Å).[20] This suggest that the interaction between the spirocarbon and F^- is weaker than that of CN^-. This weak interaction is probably the reason for almost no response of **1** against F^- in aqueous media and the different absorption spectrum of the **1**–2F^- species from the **1**–CN^- species (Fig. 1).

^{19}F NMR analysis was carried out to further clarify the structure of **1**–2F^- species. Fig. 9 shows the NMR chart of a $CDCl_3$ solution containing **1** and *n*-tetrabutylammonium fluoride (5 equiv) after UV irradiation. A new singlet signal appears at −129.8 ppm in addition to the signals for free F^- (−82.0 ppm)[21] and FHF^- dimer (−152.5 ppm)[22] formed by the reaction of F^- with water. The appearance of this singlet signal indicates that two F^- in the **1**–2F^- species are chemically equivalent. This supports the symmetrical

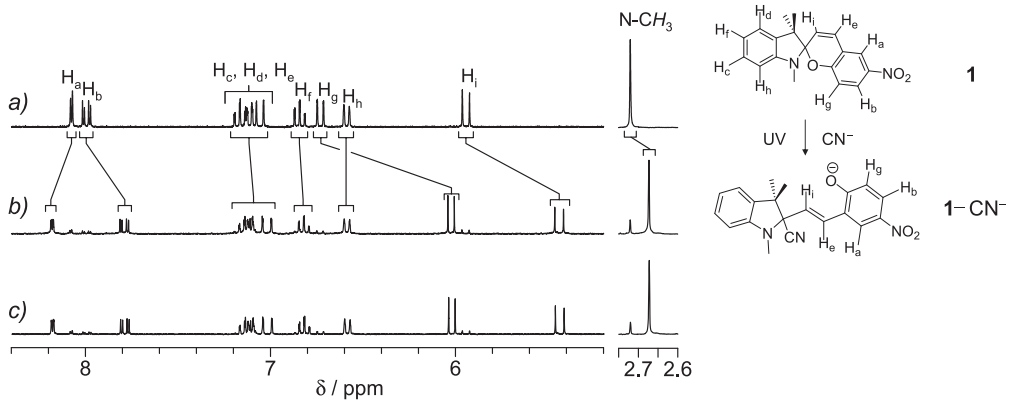

Fig. 6. ^{1}H NMR spectra (270 MHz, 30 °C, CD_3CN) of **1** (5 mM) measured (a) in the dark, (b) with 10 equiv of CN^- and UV irradiation for 10 min, and (c) after UV irradiation of the sample (b) for 1 h.

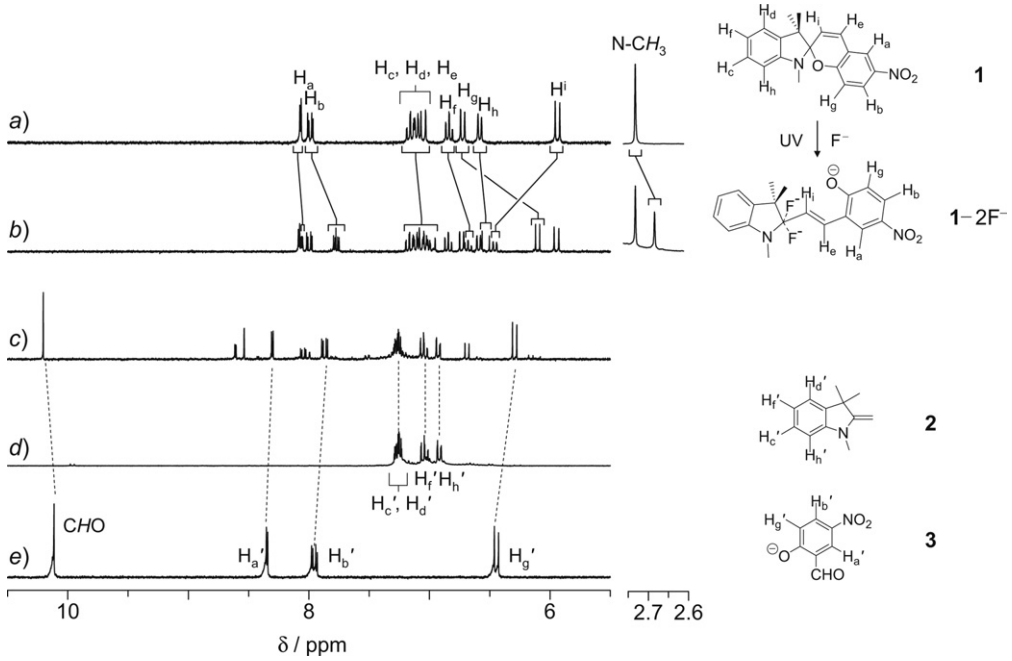

Fig. 7. ^{1}H NMR spectra (270 MHz, 30 °C, CD_3CN) of **1** (5 mM) measured (a) in the dark, (b) with 10 equiv of F^- and UV irradiation for 10 min, and (c) after UV irradiation of the sample (b) for 1 h ^{1}H NMR spectra of (d) 1,3,3-trimethyl-2-methyleneindoline, **2**, and (e) 2-formyl-4-nitro-phenol anion, **3**.

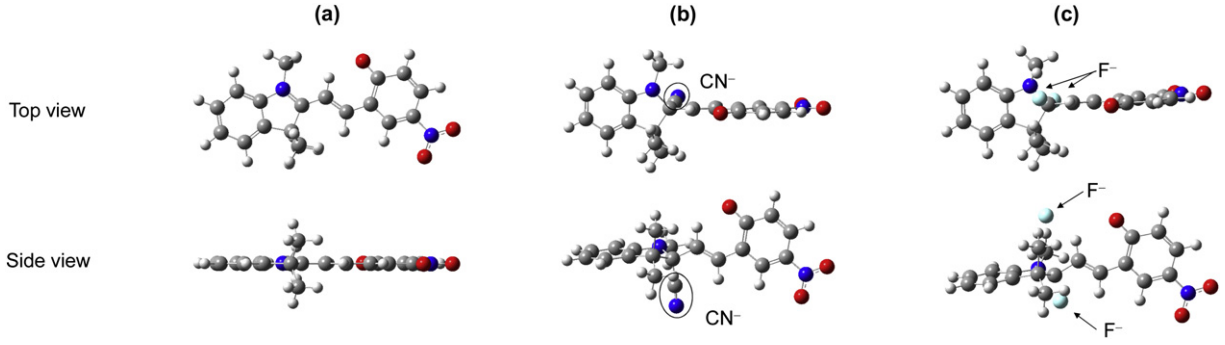

Fig. 8. Top and side views of calculated structures of (a) the MC form of **1** (B3LYP/6-31+G*), (b) **1**–CN^- species (B3LYP/6-31+G*), and (c) **1**–$2F^-$ species (B3LYP/6-31G**).

geometry of two F^- in the calculated **1**–$2F^-$ structure (Fig. 8c). This also suggests that the spirocarbon of the MC form of **1** simultaneously associates with two F^-. The isosbestic points observed in the absorption titration data with F^- (Fig. 3) is therefore due to the simultaneous interaction between **1** and two F^-.

1 associates with CN^- in a 1:1 stoichiometry, but associates with F^- in a 1:2 stoichiometry. The 1:2 association between **1** and F^- is probably due to the weak nucleophilicity of F^- as compared to CN^-;[23] two F^- are required for stabilization of the positive charge of indole moiety. The weaker association with F^- than CN^- is supported by the higher activation energy (Table 1) and the longer distance between the spirocarbon and F^- (Fig. 8). Further confirmation is made by ^{1}H NMR analysis. As reported,[24] the olefinic H_i proton of the MC form is magnetically deshielded due to the ring

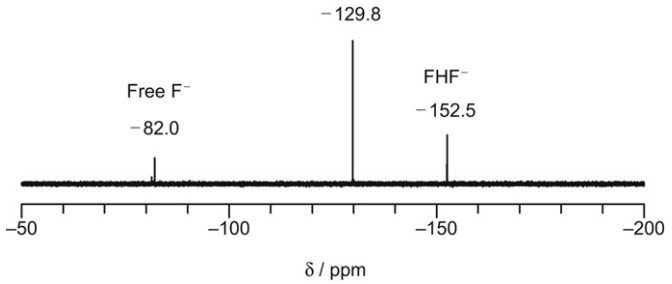

Fig. 9. ^{19}F NMR spectrum (376 MHz, 30 °C, $CDCl_3$) of **1** (30 mM) measured with 5 equiv of F^- and UV irradiation for 10 min.

current effect by the adjacent indole moiety and shifts downfield as compared to the SP form. However, as shown in Fig. 6, the H_i proton of **1** shifts upfield upon addition of CN^- and UV irradiation. This is because the interaction between the spirocarbon and CN^- leads to a decrease in electron density of the indole moiety and suppresses the ring current effect.[13] In the case of F^- (Fig. 7), the H_i proton of **1** still shifts downfield. This is probably because the decrease in electron density of the indole moiety is lower than that of CN^- due to the weak association between the spirocarbon and F^-.

2.5. Photostability of 1–CN^- and 1–$2F^-$ species

The stability of the **1**–CN^- and **1**–$2F^-$ species against UV irradiation must be noted. Fig. 10 shows the change in absorption spectra of the **1**–CN^- and **1**–$2F^-$ species in pure MeCN during UV irradiation. The spectrum of the **1**–CN^- species scarcely changes even after UV irradiation for 1 h (Fig. 10a). However, as shown in Fig. 10b, the spectrum of the **1**–$2F^-$ species red shifts with the irradiation time (427→434 nm). Figs. 6c and 7c show the ^1H NMR spectra of the **1**–CN^- and **1**–$2F^-$ species after UV irradiation for 1 h. As shown in Fig. 6c, the **1**–CN^- spectrum is similar to that obtained before irradiation (Fig. 6b), indicating that the **1**–CN^- species is stable against UV irradiation. In contrast, UV irradiation of the **1**–$2F^-$ species shows a spectrum (Fig. 7c) completely different from the spectrum obtained before irradiation (Fig. 7b). This clearly suggests that the **1**–$2F^-$ species is decomposed by UV irradiation.

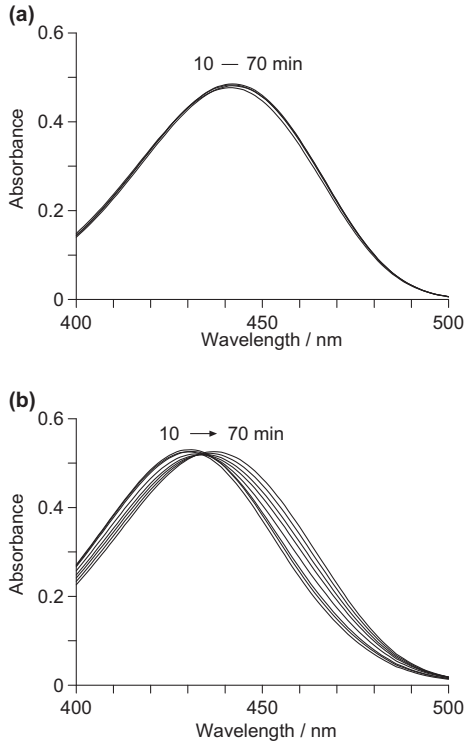

Fig. 10. Time-dependent change in absorption spectra of (a) **1**–CN^- and (b) **1**–$2F^-$ species measured in MeCN under UV irradiation (334 nm). The measurements were carried out as follows: **1** (20 μM) and CN^- or F^- (50 equiv) were stirred in MeCN under UV irradiation for 10 min to generate the respective species, and measurements were started with continued UV irradiation.

Although the decomposition product of the **1**–$2F^-$ species cannot be identified at the present stage, some of the chemical shifts of the products can be assigned. Fig. 7d and e show the ^1H NMR spectra of 1,3,3-trimethyl-2-methyleneindoline (**2**) and 2-formyl-4-nitrophenol anion (**3**), respectively, which are the precursors used for the synthesis of **1**.[13] The chemical shifts of the aromatic protons (H_c', H_d', H_f', and H_h') for **2** at 6.90–7.25 ppm are also observed in the spectrum of the decomposition product (Fig. 7c). In addition, as shown in Fig. 7e, distinctive three signals for **3** (doublet H_a', 8.35 ppm; doublet of doublets H_b', 7.96 ppm; doublet H_g', 6.44 ppm) are also observed in the spectrum of the decomposition product (Fig. 7c). These data imply that UV irradiation of the **1**–$2F^-$ species leads to a dissociation of the C=C bond of the MC form, producing the fragments containing the indole or nitroaromatic moiety. This C=C bond cleavage promoted by UV irradiation is probably due to the high electron negativity of the adjacent F atom, as is observed for related fluorinated compounds.[25] It must be noted that, as shown in the Fig. 7c, the decomposition product shows a chemical shift at lower magnetic field (10.21 ppm), which is probably assigned to the aldehyde proton as observed for compound **3**. This implies that the F^--promoted cleavage of the C=C bond followed by oxidation with molecular oxygen is involved in the decomposition pathway of the **1**–$2F^-$ species.

3. Conclusion

The detailed properties of spiropyran derivative, **1**, for anions in aqueous or organic media have been studied under UV irradiation. In aqueous media, **1** selectively interacts with CN^- (formation of **1**–CN^- species) regardless of pH and water content of the solution. The reaction is, however, suppressed by a decrease in pH and an increase in water content due to the protonation of CN^-. In contrast, in pure MeCN, addition of F^- also creates a blue-shifted absorption band as well as CN^-. This is due to the nucleophilic interaction between **1** and F^- in a 1:2 stoichiometry (formation of **1**–$2F^-$ species). The **1**–CN^- species is robust against UV irradiation. In contrast, UV irradiation of the **1**–$2F^-$ species leads to a fragmentation of the MC form of **1**, probably due to the F^--promoted C=C bond cleavage.

4. Experimental section

4.1. Materials

All of the reagents used were supplied from Wako, Aldrich, and Tokyo Kasei and used as received. Water was purified by the Milli Q system. The receptor **1** was synthesized according to the procedure described previously.[13]

4.2. Analysis

Absorption spectra were measured with magnetic stirring using a 10 mm path-length quart cell on a UV-visible photodiode-array spectrophotometer (Shimadzu; Multispec-1500) equipped with a temperature controller (Shimadzu; S-1700).[26] UV light was irradiated with a Xenon lamp (300 W; Asahi Spectra Co. Ltd.; Max-302) equipped with 334 nm band-pass filter (LX334; light intensity, 1.10 W m^{-2}).[27] ^1H NMR spectra were obtained by a JEOL JNM-

GSX270 Excalibur using TMS as an internal standard. ^{19}F NMR spectra were obtained by a Bruker DPX-400 using $CF_3C_6H_5$ (−63.9 ppm) as an external standard in $CDCl_3$.[28]

4.3. Computational details

Preliminary geometry optimizations were performed using the WinMOPAC version 3.0 software (Fujitsu Inc.) at the semiempirical PM3 level.[29] The obtained structures were fully refined with the tight convergence criteria at the DFT level with the Gaussian 03 package. Cartesian coordinates for these species are summarized in the end of Supplementary data.

Acknowledgements

This work was supported by the Grant-in-Aid for Scientific Research (No. 21760619) from the Ministry of Education, Culture, Sports, Science and Technology, Japan (MEXT). We thank Prof. Y. Tobe and Dr. K. Tahara (Osaka University) for ^{19}F NMR analysis.

Supplementary data

Figs S1–S5, and Cartesian coordinates for the MC form of **1**, **1**−CN^-, and **1**−$2F^-$ species. Supplementary data related to this article can be found online at doi:10.1016/j.tet.2010.12.021. These data include MOL files and InChiKeys of the most important compounds described in this article.

References and notes

1. For reviews: (a) Beer, P. D.; Gale, P. A. *Angew. Chem., Int. Ed.* **2001**, *40*, 486–516; (b) Suksai, C.; Tuntulani, T. *Chem. Soc. Rev.* **2003**, *32*, 192–202; (c) Gale, P. A. *Chem. Commun.* **2008**, 4525–4540; (d) Steed, J. W. *Chem. Soc. Rev.* **2009**, *38*, 506–519.
2. (a) Vázquez, M.; Fabbrizzi, L.; Tablietti, A.; Pedrido, R. M.; González-Noya, A. M.; Bermejo, M. R. *Angew. Chem., Int. Ed.* **2004**, *43*, 1962–1965; (b) Liu, X. Y.; Bai, D. R.; Wang, S. *Angew. Chem., Int. Ed.* **2006**, *45*, 5475–5478; (c) Kim, Y.; Gabbaï, F. P. *J. Am. Chem. Soc.* **2009**, *131*, 3363–3369.
3. (a) Schazmann, B.; Alhashimy, N.; Diamond, D. *J. Am. Chem. Soc.* **2006**, *128*, 8607–8614; (b) Li, Y.; Flood, A. H. *Angew. Chem., Int. Ed.* **2008**, *47*, 2649–2652; (c) Gassensmith, J. J.; Matthys, S.; Lee, J.-J.; Wojcik, A.; Kamat, P. V.; Smith, B. D. *Chem.—Eur. J.* **2010**, *16*, 2916–2921.
4. (a) Singh, N. J.; Jun, E. J.; Chellappan, K.; Thangadurai, D.; Chandran, R. P.; Hwang, I.-C.; Yoon, J.; Kim, K. S. *Org. Lett.* **2007**, *9*, 485–488; (b) Kumar, S.; Luxami, V.; Kumar, A. *Org. Lett.* **2008**, *10*, 5549–5552; (c) Goswami, S.; Chakrabarty, R. *Tetrahedron Lett.* **2009**, *50*, 5994–5997.
5. (a) Lu, H.; Xu, W.; Zhang, D.; Zhu, D. *Chem. Commun.* **2005**, 4777–4779; (b) Jang, Y. J.; Jun, E. J.; Lee, Y. J.; Kim, Y. S.; Kim, J. S.; Yoon, J. *J. Org. Chem.* **2005**, *70*, 9603–9606; (c) Caltagirone, C.; Gale, P. A.; Hiscock, J. R.; Brooks, S. J.; Hursthouse, M. B.; Light, M. E. *Chem. Commun.* **2008**, 3007–3009.
6. (a) Labande, A.; Astruc, D. *Chem. Commun.* **2000**, 1007–1008; (b) Curiel, D.; Beer, P. D. *Chem. Commun.* **2005**, 1909–1911; (c) Kim, H. J.; Bhuniya, S.; Mahajan, R. K.; Puri, R.; Liu, H.; Ko, K. C.; Lee, J. Y.; Kim, J. S. *Chem. Commun.* **2009**, 7128–7130.
7. (a) Koenig, R. *Science* **2000**, *287*, 1737–1738; (b) Baud, F. *Hum. Exp. Toxicol.* **2007**, *26*, 191–201.
8. *Guidelines for Drinking-Water Quality*; World Health Organization: Geneva, 1996.
9. (a) Chung, Y. M.; Raman, B.; Kim, D.-S.; Ahn, K. H. *Chem. Commun.* **2006**, 186–188; (b) Parab, K.; Venkatasubbaiah, K.; Jäkle, F. *J. Am. Chem. Soc.* **2006**, *128*, 12879–12885; (c) Hong, S.-J.; Yoo, J.; Kim, S.-H.; Kim, J. S.; Yoon, J.; Lee, C.-H. *Chem. Commun.* **2009**, 189–191; (d) Park, I. S.; Jung, Y.-S.; Lee, K.-J.; Kim, J.-M. *Chem. Commun.* **2010**, *46*, 2859–2861.
10. (a) Lou, X.; Zhang, L.; Qin, J.; Li, Z. *Chem. Commun.* **2008**, 5848–5850; (b) Jamkratoke, M.; Ruangpornvisuti, V.; Tumcharern, G.; Tuntulani, T.; Tomapatanaget, B. *J. Org. Chem.* **2009**, *74*, 3919–3922; (c) Lin, Y.-C.; Chen, C.-T. *Org. Lett.* **2009**, *11*, 4858–4861; (d) Agou, T.; Sekine, M.; Kobayashi, J.; Kawashima, T. *Chem.—Eur. J.* **2009**, *15*, 5056–5062.
11. (a) Ros-Lis, J. V.; Martínez-Máñez, R.; Soto, J. *Chem. Commun.* **2005**, 5260–5262; (b) Hudnall, T. W.; Gabbaï, F. P. *J. Am. Chem. Soc.* **2007**, *129*, 11978–11986; (c) Lee, K.-S.; Kim, H.-J.; Kim, G.-H.; Shin, I.; Hong, J.-I. *Org. Lett.* **2008**, *10*, 49–51; (d) Jo, J.; Lee, D. *J. Am. Chem. Soc.* **2009**, *131*, 16283–16291.
12. (a) Chow, C.-F.; Lam, M. H. W.; Wong, W.-Y. *Inorg. Chem.* **2004**, *43*, 8387–8393; (b) Badugu, R.; Lakowicz, J. R.; Geddes, C. D. *Dyes Pigm.* **2005**, *64*, 49–55; (c) Badugu, R.; Lakowicz, J. R.; Geddes, C. D. *J. Am. Chem. Soc.* **2005**, *127*, 3635–3641; (d) Tomasulo, M.; Raymo, F. M. *Org. Lett.* **2005**, *7*, 4633–4636; (e) Tomasulo, M.; Sortino, S.; White, A. J. P.; Raymo, F. M. *J. Org. Chem.* **2006**, *71*, 744–753; (f) Cho, D.-G.; Kim, J. H.; Sessler, J. L. *J. Am. Chem. Soc.* **2008**, *130*, 12163–12167; (g) Sun, Y.; Liu, Y.; Chen, M.; Guo, W. *Talanta* **2009**, *80*, 996–1000; (h) Männel-Croisé, C.; Zelder, F. *Inorg. Chem.* **2009**, *48*, 1272–1274; (i) Lou, X.; Qiang, L.; Qin, J.; Li, Z. *ACS Appl. Mater. Interfaces* **2009**, *1*, 2529–2535; (j) Saha, S.; Ghosh, A.; Mahato, P.; Mishra, S.; Mishra, S. K.; Suresh, E.; Das, S.; Das, A. *Org. Lett.* **2010**, *12*, 3406–3409.
13. Shiraishi, Y.; Adachi, K.; Itoh, M.; Hirai, T. *Org. Lett.* **2009**, *11*, 3482–3485.
14. Shiraishi, Y.; Itoh, M.; Hirai, T. *Phys. Chem. Chem. Phys.* **2010**, *12*, 13737–13745.
15. Benesi, H. A.; Hildebrand, J. H. *J. Am. Chem. Soc.* **1949**, *71*, 2703–2707.
16. Kieβwetter, R.; Pustet, N.; Brandl, F.; Mannschreck, A. *Tetrahedron: Asymmetry* **1999**, *10*, 4677–4687.
17. Yagi, S.; Nakamura, S.; Watanabe, D.; Nakazumi, H. *Dyes Pigm.* **2009**, *80*, 98–105.
18. (a) Frisch, M. J.; Trucks, G. W.; Schlegel, H. B.; Scuseria, G. E.; Robb, M. A.; Cheeseman, J. R., Jr.; Montgomery, J. A.; Vreven, T.; Kudin, K. N.; Burant, J. C.; Millam, J. M.; Iyengar, S. S.; Tomasi, J.; Barone, V.; Mennucci, B.; Cossi, M.; Scalmani, G.; Rega, N.; Petersson, G. A.; Nakatsuji, H.; Hada, M.; Ehara, M.; Toyota, K.; Fukuda, R.; Hasegawa, J.; Ishida, M.; Nakajima, T.; Honda, Y.; Kitao, O.; Nakai, H.; Klene, M.; Li, X.; Knox, J. E.; Hratchian, H. P.; Cross, J. B.; Bakken, V.; Adamo, C.; Jaramillo, J.; Gomperts, R.; Stratmann, R. E.; Yazyev, O.; Austin, A. J.; Cammi, R.; Pomelli, C.; Ochterski, J. W.; Ayala, P. Y.; Morokuma, K.; Voth, G. A.; Salvador, P.; Dannenberg, J. J.; Zakrzewski, V. G.; Dapprich, S.; Daniels, A. D.; Strain, M. C.; Farkas, O.; Malick, D. K.; Rabuck, A. D.; Raghavachari, K.; Foresman, J. B.; Ortiz, J. V.; Cui, Q.; Baboul, A. G.; Clifford, S.; Cioslowski, J.; Stefanov, B. B.; Liu, G.; Liashenko, A.; Piskorz, P.; Komaromi, I.; Martin, R. L.; Fox, D. J.; Keith, T.; Al-Laham, M. A.; Peng, C. Y.; Nanayakkara, A.; Challacombe, M.; Gill, P. M. W.; Johnson, B.; Chen, W.; Wong, M. W.; Gonzalez, C.; Pople, J. A. *Gaussian 03, Revision B.05*; Gaussian: Wallingford CT, 2004; (b) Dennington, R., II; Keith, T.; Millam, J.; Eppinnett, K.; Hovell, W. L.; Gilliland, R. *GaussView, Version 3.09*; Semichem: Shawnee Mission, KS, 2003.
19. Pyykkö, P.; Atsumi, M. *Chem.—Eur. J.* **2009**, *15*, 186–197.
20. (a) Batsanov, S. S. *Inorg. Mater.* **2001**, *37*, 871–885; (b) Wright, T. G.; Breckenridge, W. H. *J. Phys. Chem. A* **2010**, *114*, 3182–3189.
21. Shibato, A.; Itagaki, Y.; Tayama, E.; Hokke, Y.; Asao, N.; Maruoka, K. *Tetrahedron* **2000**, *56*, 5373–5382.
22. Flemming, J. P.; Pilon, M. C.; Borbulevitch, O. Y.; Antipin, M. Y.; Grushin, V. V. *Inorg. Chim. Acta* **1998**, *280*, 87–98.
23. Kim, D.-S.; Chung, Y.-M.; Jun, M.; Ahn, K. H. *J. Org. Chem.* **2009**, *74*, 4849–4854.
24. (a) Parker, W. O., Jr.; Hobley, J.; Malatesta, V. *J. Phys. Chem. A* **2002**, *106*, 4028–4031; (b) Machitani, K.; Nakamura, M.; Sakamoto, H.; Ohata, N.; Masuda, H.; Kimura, K. *J. Photochem. Photobiol., A* **2008**, *200*, 96–100.
25. (a) Hackett, P. A.; Weinberg, E.; Gauthier, M.; Willis, C. *Chem. Phys. Lett.* **1981**, *82*, 89–91; (b) Maricq, M. M.; Szente, J. J. *J. Phys. Chem.* **1992**, *96*, 10862–10868; (c) Láska, L.; Krása, J.; Juha, L. *Chem. Phys.* **1993**, *172*, 377–385; (d) Rattigan, O. V.; Rowley, D. M.; Wild, O.; Jones, R. L. *J. Chem. Soc., Faraday Trans.* **1994**, *90*, 1819–1829.
26. Shiraishi, Y.; Miyamoto, R.; Hirai, T. *Langmuir* **2008**, *24*, 4273–4279.
27. Shiraishi, Y.; Miyamoto, R.; Hirai, T. *Org. Lett.* **2009**, *11*, 1571–1574.
28. Nakaike, Y.; Hayashi, D.; Nishiwaki, N.; Tobe, Y.; Ariga, M. *Org. Biomol. Chem.* **2009**, *7*, 325–334.
29. Shiraishi, Y.; Saito, N.; Hirai, T. *J. Am. Chem. Soc.* **2005**, *127*, 8304–8306.